ELSEVIER

Journal of Nuclear Materials 248 (1997) 268–274

journal of nuclear materials

Section 11. Cladding corrosion under irradiation

Irradiation effects on corrosion of zirconium alloy claddings

Florence Lefebvre, Clément Lemaignan *

Commissariat à l'Energie Atomique, CEA-Grenoble DTP / SECC, 17 Avenue des Martyrs, 38054 Grenoble cedex 9, France

Abstract

Under irradiation, the corrosion rate of Zircaloy elements is known to be increased due to the combination of factors. This paper is a review of the recent work performed to analyze the contribution of the major physical phenomena involved in this increase in corrosion rate: the irradiation induced changes in microstructure, the thermo-hydraulic conditions, including associated chemical changes, and the effect of irradiation on the corrosion process itself (radiolysis in the coolant and in the oxide layer). © 1997 Elsevier Science B.V.

1. Introduction

The corrosion rate of Zr alloys is one of the major controlling parameters for the design of in-core components of water reactor fuel elements [1]. The tendency for higher discharge burn up of the fuel has therefore raised a large amount of analytical or global R&D work in this area [2]. Without irradiation, the physical mechanisms controlling the corrosion rate of Zr alloys become more and more understood, however a large number of individual steps and their interactions remain unclear [3]. The situation is such that a prediction of the corrosion rate of a new alloy or microstructure under a given oxidizing condition is still speculative. For in reactor corrosion, the situation is even worst. Indeed, the effects of thermal flux, coolant chemistry or irradiation damage on the structure of the alloys, on the zirconia layer or on water radiochemistry, introduce another level of complexity [3].

The aim of this paper is to present recent results related to these phenomena and to discuss them in conjunction with similar work performed thought out the world in this field. Due to the large differences in behavior of the different type of Zr alloys, this analysis will be restricted to the Zircaloy family. The following two topics will be specially detailed: (i) Irradiation damage on the alloys and the effects of the microstructure changes, (ii) Effect of irradiation on the coolant or on the ZrO_2 (radiolysis).

* Corresponding author. Tel.: +33-4 76 88 44 71; fax: +33-4 76 88 51 51; e-mail: lemaignan@cea.fr.

2. Effects of irradiation damage on corrosion mechanisms of Zircaloy

2.1. Second phase evolution

The microstructure of the Zircaloy consists of a Zr base, hcp matrix with Sn and O in solid solution. Fe, Cr and Ni were added early for improving the corrosion behavior of the alloy. These transition elements are almost insoluble in the matrix and precipitate as Zr_2(Ni, Fe) or Zr(Fe, Cr)$_2$ phases. The size distribution and exact chemical composition of these precipitates are strongly dependant of the thermo-mechanical processing history [4]. Various cumulative annealing parameters have been developed to account for the observed distributions. Since precipitates are very important for the corrosion behavior, they have been studied in detail [5,6] and their distribution and size have been clearly demonstrated to control the corrosion behavior. However, it remains not perfectly understood why a better corrosion resistance is obtained for BWR [5] with small precipitates, while the reverse is true for PWR conditions [1,7,8]. In addition, these precipitates could act, first, as cathodic sites inducing an enhanced passivation of the Zr matrix and, then, as protective anodic sites, as proposed recently, when a low corrosion rate was obtained by galvanic coupling of a precipitate free Zr alloy plate on a large Zr(Fe, Cr)$_2$ intermetallic compound [9].

Under irradiation, the precipitates undergo structural transformations, the nature of which being temperature and flux dependant [10,11]. At the lowest temperature found in power reactors, and only for the Zr(Fe, Cr)$_2$ phase, an

PII S0022-3115(97)00123-2

amorphous transformation occurs that starts at the matrix-precipitate interface and grows inward at a constant rate, leading to a 'duplex' structure of the precipitates. Simultaneously Fe, and to a lesser exten Cr, is dissolving in the matrix. For very high doses, the precipitates may be completely dissolved. At higher temperature (when thick oxide layers are present) the dissolution may occur without amorphous transformation [12–14].

This transformation and dissolution could be partially at the origin of the increase found in corrosion rate at high burn-up (BU) [7]. Corrosion experiments performed either without irradiation on previously irradiated material or in reactor confirm a higher corrosion rate of Zircaloy after high irradiation doses [15–17]:

Zircaloy-4 cladding from fuel rods irradiated in the BR3 reactor were machined in hot cell to remove the oxide layer, and exposed to a standard corrosive environment (15 MPa steam at 673 K) to assess the impact of irradiation induced changes in microstructure on corrosion [17]. It was found that when the samples had received a high dose to induce advanced dissolution of the precipitates, a higher corrosion rate was observed, compared to non-irradiated materials. This is also the case for high BU fuel cladding corrosion rate during irradiation. Indeed, a transition is observed at high burn-up in reactors: the corrosion rates are increasing sharply to values that cannot be explained by simple extrapolation of early corrosion behavior under irradiation. Many cases of such late increase have been reported in both, PWR and BWR environments (e.g., [5,7]).

In order to understand the specific aspect of microstructure changes on the corrosion mechanisms, the behavior of the precipitates and their interactions with the growing oxide have been analyzed using analytical TEM on thin foils prepared at different depths in oxide layers obtained on non-irradiated material [18], on cladding pre-irradiated and oxidized without irradiation [19–21] or on cladding oxidized in reactor [17].

An important observation is the delayed oxidation of the precipitates with respect to the matrix, as presented in Fig. 1. This behavior can be explained by the gradient in oxygen potential through the oxide layer. Indeed, $P(O_2)$ is expected to be too low close to the metal–oxide interface for the oxidation of Fe or Cr to occur. The oxidation of the precipitates could therefore start only in the middle of the dense oxide layer. An important consequence is that, since the oxidation of the metallic precipitates is observed to occur simultaneously to an Fe depletion, these precipitates, embedded in the zirconia deeper layer, act as sources of Fe. Thus, close to the metal–oxide no iron is available for zirconia doping, while at several microns away from the interface, the redistribution of Fe in the zirconia surrounding former precipitates leads to local significant doping effects. The presence of Fe in zirconia is observed to be linked to the stabilization, by chemical doping, of the tetragonal phase of the zirconia. Thus, close to the metal–oxide interface, the dense oxide layer is found to be mostly tetragonal due to the large compressive strains associated with the oxide growth and to contain almost no iron doping. Several microns away from the interface, due to the delayed oxidation of the precipitates, associated with a delayed iron redistribution in the surrounding oxide, the allotropic transformation from the tetragonal to monoclinic phase can be locally postponed. This local chemical stabilization of the tetragonal phase depends on the extent of iron redistribution. Without irradiation the Fe redistribution remains rather localized and numerous small areas (1 μm large) of stabilized tetragonal zirconia can be observed sputtered in the oxide layer at several microns away from the metal–oxide interface.

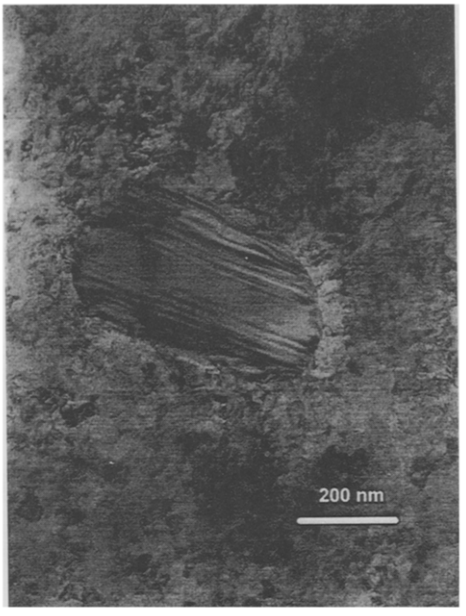

Fig. 1. Non-oxidized precipitate found in the dense layer of an oxide grown in autoclave at 673 K.

In the case of irradiated material, due to the irradiation induced precipitate evolution in the metallic matrix, the precipitate state, when embedded in the oxide, varies with the irradiation dose. At the beginning of life, the microstructure is basically unchanged and the precipitate oxidation behavior is similar to that of non-irradiated material. The Fe redistribution is however observed to be enhanced under irradiation leading to much larger areas of stabilized tetragonal zirconia (up to several μm large). At higher doses, metallic precipitates contain lower amounts of Fe and zirconium solid solution is enriched in Fe. Thus, close to the metal–oxide interface, zirconia can be significantly doped with Fe and due, to the small amount of Fe available in the precipitate, the stabilization process previously described cannot occur anymore.

The irradiation induced evolution of the metallic alloy appears to have direct consequences on the oxide structure and particularly, to generate significant microstructural heterogeneity trough the oxide which natures and distributions varies with the irradiation dose.

As it will be shown later on, the areas of high tetragonal content could have a reactivity different from those entirely monoclinic. Their size and distribution can thus be associated with the tendency of the oxide to develop a fine network of micro-porosities or to remain protective. In the other hand, the progressive Fe doping of the dense zirconia located at the immediate vicinity of the metal–oxide interface could also contribute to decrease its protective character and to increase the corrosion rate.

2.2. Oxide layer growth

In addition to this simple analysis, the effect of the fast neutron flux and irradiation damage on the oxide should be considered. The comparisons of the oxide microstructure and of the chemistry around precipitates, on oxidized layers formed in autoclave on both non-irradiated and irradiated metallic samples or directly in reactor (Fig. 2), lead to the following conclusions [17,19,20].

· On non-irradiated material, the oxide is growing on the matrix with strong preferential orientation relationships, leading to a strongly textured zirconia layer (Fig. 2a). Few localized areas consist of crystallites smaller than elsewhere ($\bar{d} \approx 10$ nm compared to $\bar{d} \approx 50$ nm) without

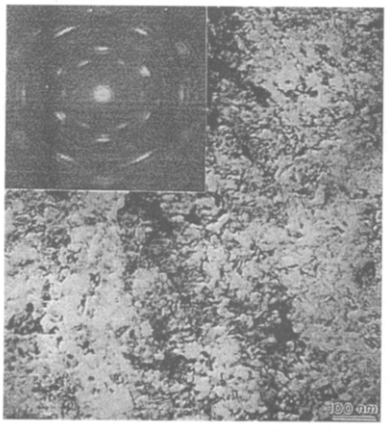

a) dense, fine and compact monoclinic / tetragonal grains (usually columnar)

b) large unstable grains observed on oxide grown under irradiation.

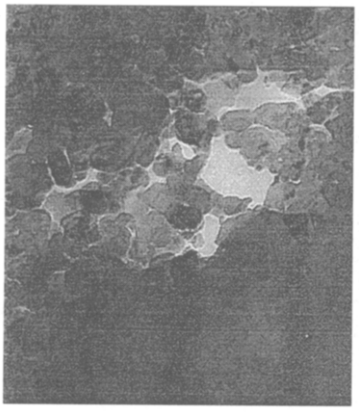

c) loose, granular oxide obtained in case of increased corrosion rate

Fig. 2. Various aspects of the zirconia found in the oxide layers: (a) dense, fine and compact monoclinic/tetragonal grains (usually columnar); (b) large unstable grains observed on oxide grown under irradiation; (c) loose, granular oxide obtained in case of increased corrosion rate.

any preferred orientation. These orientations change continuously throughout the oxide thickness leading to a texture mostly fibrous in nature.

· For in-reactor grown corrosion layers [17,20], a tendency is observed for coarser oxide crystallites and less frequent areas showing a marked common orientation. The fast neutron flux seems to favor the presence of an amorphous zirconia layer close to the metal–oxide interface. The presence of this amorphous layer may inhibit the epitaxy of the zirconia layer on the matrix, leading to the observed higher degree of randomness in the orientation of the monoclinic or tetragonal crystallites. In addition, large grains are found in the middle of the oxide layer (Fig. 2b), showing that a recrystallization process has occurred during in-reactor corrosion. The tendency to an additional recrystallization in the thin foil, under the electron beam, during TEM observation confirms the contribution of a specific mechanism of phase transformation associated with the high amount of energy stored in the lattice due to irradiation damage. This recrystallization process produces large monoclinic crystallites, with some intergranular cracking. Thus it seems to be clearly different from the recrystallization process giving rise to the 'granular', loose, oxide structure (Fig. 2c), that could be the result of a dissolution/re-precipitation process [17,22,23].

In addition to the irradiation damage leading, in particular, to this recrystallization of the zirconia, the fast neutron flux induces a ballistic diffusion of the Fe and Cr present

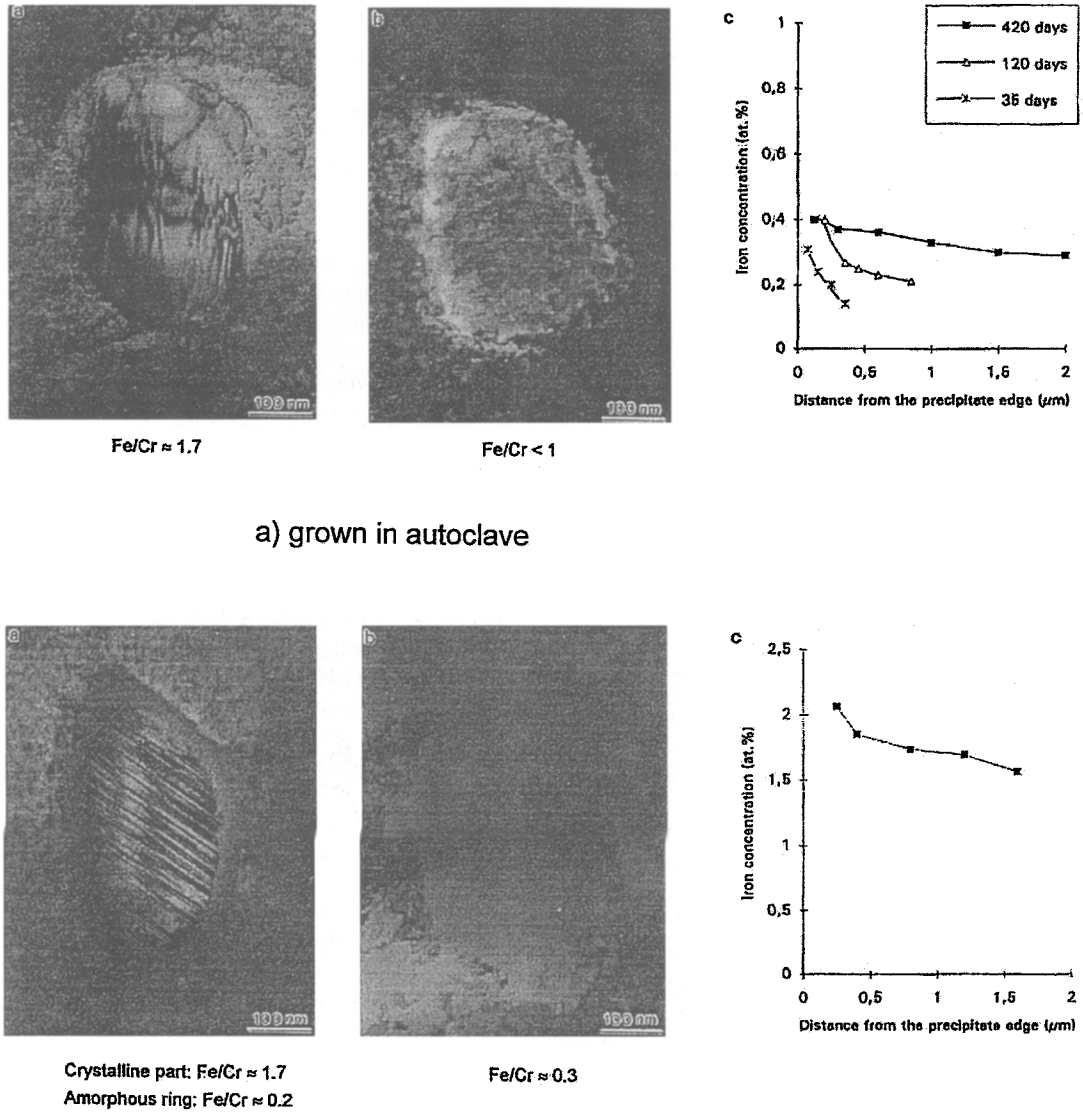

Fig. 3. Fe distribution in the vicinity of a precipitate in the oxide layer. (a) grown in autoclave (b) grown in reactor.

in the precipitates. Indeed, the diffusion of these elements in the zirconia surrounding oxidized precipitates is clearly more limited during autoclave testing, compared to oxidation in reactor (Fig. 3). As previously discussed, this enhanced diffusion has two main consequences: it accelerates the precipitates depletion, reducing the time during which precipitates may act as a Fe reservoirs and, by the same process, as long as precipitates are not sufficiently depleted, it spreads Fe around the precipitates, increasing locally the stability of the tetragonal phase. There are evidences, on bulk zirconia, of a strong interaction between tetragonal zirconia and hot water leading to the destabilization of the tetragonal form into the monoclinic one simultaneously to a dissolution/re-precipitation process [24,25]. These areas of high tetragonal content due to Fe stabilization could thus undergo a similar transformation. This hypothesis appears to be consistent with the observation, several microns away from the metal–oxide interface, of areas of oxide having an extremely porous structure (similar to Fig. 2c) and a high Fe content. The irradiation-enhanced mobility of Fe in the oxide layer seems thus to contribute to decrease the protective character of the oxide layer, leading to a lower corrosion resistance under irradiation.

3. Chemistry of the coolant and radiolysis

3.1. Effect of coolant chemistry

In reactor the thermo-hydraulic conditions are somewhat different from that found during autoclave testing: the heat flux and the flow rate on one hand and the two phase conditions (BWR and nucleate boiling in hot PWRs) on the other, lead to specific chemical boundary conditions for in-reactor corrosion. The effect of heat flux can adequately be analyzed using out of reactor corrosion loops, in which thermo-hydraulic conditions may be very similar to the power reactor conditions and, if requested, slightly outside the normal ranges in order to analyze any induced effect [26]. This type of equipment allowed to determine the effect of LiOH on zirconia microstructure and to compare the microstructure obtained in these conditions with the one grown directly in LiOH rich water autoclave [23]. The detrimental effect, on corrosion rate, of high LiOH content, specially the PWR water in thick oxide film porosities or in nucleate boiling conditions, has been acknowledged since a long time [27,28] and is now under close investigation [23,29,30]. An enhanced dissolution kinetics of the tetragonal phase has been proposed [31], but a clear understanding of the physical processes involved is however still lacking.

3.2. Radiolysis

Following an early proposal on a thick film effect on irradiation induced corrosion of Zr alloys [32], it has been proposed that a local radiolysis could occur under irradiation in the porous part of thick zirconia layers, with high values in front of emitters [33]. Further analysis of the energy deposition rate have shown an increase in radiolysis of the water close to the oxide interfaces, due to an additional secondary electron flux arising from zirconia [34]. In order to analyze the potential effect of any local energy deposition on corrosion rate of the cladding in a PWR environment, an experiment has been set up, where a short fuel rod has been irradiated in a pressurized loop, with local sources of β^- electrons placed at various positions in front of the fuel rod [35].

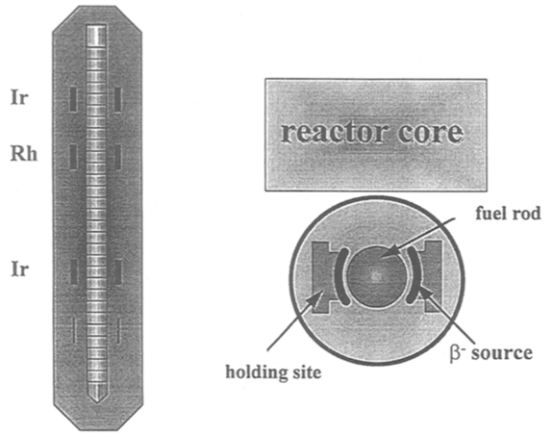

Fig. 4. Schematic view of the irradiation device used to analyze the effect of local radiolysis on corrosion rate.

Using a new fuel cladding tube already oxidized to 6 μm in an out of reactor loop, a fuel rod has been constructed and irradiated in a nucleate boiling device in the Siloé reactor for 77 days at a maximum linear power of 45 kW m^{-1}. The device was equipped with insulating holders loaded with iridium and rhodium foils. One holder was free of materials to confirm the absence of any thermo-hydraulic perturbations responsible for a corrosion rate increase. The sketch of this device and its fuel rod is given in Fig. 4. Due to the neutron capture of the β emitters, the linear power was slightly reduced locally in front of these sources. The increase of energy deposition rate was increased only by a factor of 1.25 (from 6 W g^{-1} outside the sources, to 8.5 W g^{-1} in front of Rh sources). After irradiation the oxide layer thickness, shown in Fig. 5, is weakly dependant of the axial position and no specific increase can be found in front of the sources.

This result seems to be in direct disagreement with a recent experiment performed with a similar aim in a BWR environment [36,37], where localized enhanced corrosion was found in front of Pt foils. However several differences have to be highlighted between these two experiments. The main difference concerns the coolant conditions: in the PWR device LiOH = 2 ppm was added as well as H_2 (3–5 ppm) and O_2 was maintained at 5 ppb (note the absence of

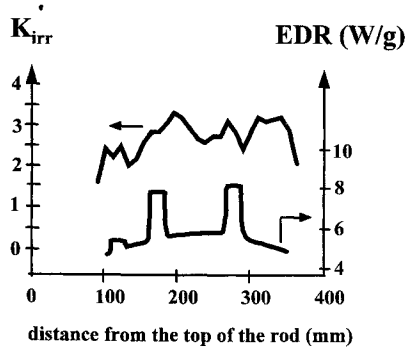

Fig. 5. Relative oxide thickness along the fuel rod after 77 days in the irradiation rig. K_{irr} is the measured oxide thickness divided by the thickness expected without irradiation. EDR is the energy deposition rate.

boron). The BWR device was in two phase flow and the oxygen content was comparatively high (300 ppb) and had a coolant flow 10 times higher. The lack of any detectable radiolysis effect in the Siloé experiment was tentatively analyzed by a possible overwhelming by other irradiation effects in the oxide (such as enhanced diffusion of the oxygenated species or higher conductivity due to electron-hole defects). More likely, water radiolysis efficiency has been inhibited compared to the BWR experiment, due to the low amount of oxygen in the water and the large additions of hydrogen.

Indeed, slight radiolysis effects were found in other experiments, specially during autoclave corrosion or electrochemistry testings in the vicinity of β emitters performed with aerated water and no addition of hydrogen [35]. The contribution of the water chemistry appears as a major parameter controlling the intensity of any radiolytic effect.

4. Conclusions

The effect of irradiation on the corrosion kinetics of Zircaloy has been analyzed using analytical TEM for characterizing microstructural evolution of the zirconia grown out of- and in-reactor and their consequences on the corrosion rate. Clear differences are found in the microstructure that can be tentatively explained either by the irradiation induced evolution of microstructure (amorphous transformation of the precipitates and Fe re-solution) or by the radiation damage in the oxide layer during nucleation on the Zr matrix or during growth in the dense layer. In addition, a dissolution/re-precipitation mechanism of the tetragonal zirconia induced by hot water and enhanced by high LiOH concentration in the coolant would be consistent to explain the acceleration of the corrosion rate in reactor.

An experiment has been set up in which a short fuel rod has been irradiated in a PWR environment in front of β emitting foils. In contrary to a similar experiment performed in BWR conditions, no local corrosion enhancement was found. This result tends to emphasize the low tendency for local corrosion acceleration induced by β radiolysis without two-phase flow conditions and/or without a sufficient oxygen content.

Acknowledgements

The basis of this paper is a review of the work undertaken since several years at CEA Grenoble, with Xavière Iltis, Christian Regnard and Raphaël Salot. The authors gratefully acknowledge their contributions to a better understanding of the mechanisms of enhanced corrosion under irradiation.

References

[1] F. Garzarolli, R. Holzer, Nucl. Energy 31 (1992) 65.
[2] M. Morel, J. Thomazet, A. Netter, G. Kopff, Technique and method for upgrading corrosion performance though Fragema fuel experience feedback, Int. Topical Meeting on Light Water Reactor Fuel Performance, ANS ENS, West Palm Beach, FL, 1994, pp. 296–302.
[3] Corrosion of Zirconium in nuclear power plants, IAEA, Vienna, Austria, 1993.
[4] J.P. Gros, J.F. Wadier, J. Nucl. Mater. 172 (1990) 85.
[5] F. Garzarolli, R. Schumann, E. Steinberg, Corrosion optimized Zircaloy for BWR fuel elements, 10th Int. Symp. on Zirconium in the Nuclear Industry, Baltimore, MD, ASTM STP 1245, 1994, pp. 709–723.
[6] Y. Isobe, Y. Matsuo, Y. Mae, Micro-characterization of corrosion resistant Zr-based alloys, 11th. Int. Symp. on Zirconium in the Nuclear Industry, Garmisch-Partenkirchen, FRG, ASTM-STP 1295, 1996, pp. 437–449.
[7] L.F.P. Van Swam, S.H. Shann, The corrosion of Zircaloy-4 fuel cladding in pressurized water reactor, 9th Int. Symp. on Zirconium in the Nuclear Industry, Kobe, Japan, ASTM STP 1132, 1991, pp. 758–781.
[8] J.P. Mardon, D. Charquet, J. Senevat, Optimisation of PWR behavior of stress-relieved Zircaloy-4 cladding tubes by improving the manufacturing and inspection process, 10th Int. Symp. on Zirconium in the Nuclear Industry, Baltimore, MD, ASTM STP 1245, 1994, pp. 328–348.
[9] Y. Isobe, T. Murai, Y. Mae, Anodic protection of precipitates in aqueous corrosion of Zircaloy, 11th Int. Symp. on Zirconium in the Nuclear Industry, Garmisch-Partenkirchen, FRG, ASTM-STP 1295, 1996, pp. 203–217.
[10] Y. Etoh, S. Shimada, J. Nucl. Mater. 200 (1993) 59.
[11] W.J.S. Yang, J. Nucl. Mater. 158 (1988) 71.
[12] D. Gilbon, C. Simonot, Effect of irradiation on the microstructure of Zircaloy-4, 10th Int. Symp. on Zirconium in the Nuclear Industry, Baltimore, MD, ASTM STP 1245, 1994, pp. 521–548.
[13] D. Pecheur, F. Lefebvre, A.T. Motta, C. Lemaignan, D. Charquet, J. Nucl. Mater. 205 (1993) 445.
[14] F. Garzarolli, W. Goll, A. Seibold, I. Ray, Effect of PWR

irradiation on size, structure and composition of intermetallic precipitates of Zr alloys, 11th Int. Symp. on Zirconium in the Nuclear Industry, Garmisch-Partenkirschen, ASTM STP 1295, 1996, pp. 541–556.

[15] P.Y. Huang, S.T. Mahmood, R.B. Adamson, Effect of thermomechanical porcessing on in-reactor and post-irradiation mechanical properties of Zircaloy-2, 11th. Int. Symp. on Zirconium in the Nuclear Industry, Garmisch-Partenkirchen, FRG, ASTM-STP 1295, 1996, pp. 726–757.

[16] B. Cheng, R.M. Kruger, R.B. Adamson, Corrosion behaviour of irradiated Zircaloy, 10th Int. Symp. on Zirconium in the Nuclear Industry, Baltimore, MD, ASTM STP 1245, 1994, pp. 400–418.

[17] X. Iltis, F. Lefebvre, C. Lemaignan, Microstructure evolutions and iron redistribution in Zircaloy oxide layers: comparative effects of irradiation flux and irradiation damages, 11th Int. Symp. on Zirconium in the Nuclear Industry. Garmisch-Partenkirchen, FRG, ASTM-STP 1295, 1996, pp. 242–264.

[18] D. Pecheur, F. Lefebvre, A.T. Motta, C. Lemaignan, J.F. Wadier, J. Nucl. Mater. 189 (1992) 318.

[19] X. Iltis, F. Lefebvre, C. Lemaignan, J. Nucl. Mater. 224 (1995) 109.

[20] X. Iltis, F. Lefebvre, C. Lemaignan, J. Nucl. Mater. 224 (1995) 121.

[21] D. Pecheur, F. Lefebvre, A.T. Motta, C. Lemaignan, D. Charquet, Oxidation of Inter metallic precipitates in Zircaloy 4: Impact of irradiation, 10th Int. Symp. on Zirconium in the Nuclear Industry, Baltimore, MD, ASTM STP 1245, 1994, pp. 687–708.

[22] H.J. Beie, A. Mitwalsky, F. Garzarolli, H. Ruhmann, H.J. Sell, Examinations of the corrosion mechanism of zirconium alloys, 10th Int. Symp. on Zirconium in the Nuclear Industry, Baltimore, MD, ASTM STP 1245, 1994, pp. 615–643.

[23] D. Pecheur, E. Picard, P. Billot, Microstructure of oxide films formed during the waterside corrosion of Zry 4 cladding in a lithiated environment, 11th Int. Symp. on Zirconium in the Nuclear Industry, Garmisch-Partenkirchen, FRG, ASTM-STP 1295, 1996, pp. 94–113.

[24] T. Sato, M. Shimada, J. Am. Ceram. Soc. 68 (1985) 356.

[25] T. Sato, S. Ohtaki, T. Endo, M. Shimada, J. Am. Ceram. Soc. 68 (1985) C320.

[26] P. Billot, P. Beslu, A. Giordano, J. Thomazet, Development of a mechanistic model to adress the external corrosion of the Zircaloy claddings in PWRs, ASTM-STP 1023, 1989, pp. 165–184.

[27] S.G. McDonald, G.P. Sabol, J.D. Sheppard, Effect of lithium hydroxide on the corrosion behaviour of Zircaloy-4, 6th Int. Symp. on Zirconium in the Nuclear Industry, Vancouver, BC, Canada, ASTM STP 824, 1984, pp. 519–530.

[28] H. Coriou, L. Grall, J. Meunier, H. Willermoz, J. Nucl. Mater. 7 (1962) 320.

[29] B. Cox, M. Ungurelu, Y. Wong, C. Wu, Mechanisms of LiOH degradation and H_3BO_3 repair in ZrO_2 films, 11th Int. Symp. on Zirconium in the Nuclear Industry, Garmisch-Partenkirchen, FRG, ASTM-STP 1295, 1996, pp. 114–136.

[30] N. Ramasubramanian, P.V. Balakrishnan, Aqueous chemistry of LiOH and Boric acid on corrosion of Zircaly-4 and Zr–2.5Nb alloys, 11th Int. Symp. on Zirconium in the Nuclear Industry, Garmisch-Partenkirchen, FRG, ASTM-STP 1295, 1996, pp. 378–399.

[31] B. Cox, J. Nucl. Mater. (1996), to be published.

[32] A.B. Johnson, Jr., Thick film effects in the oxidation and hydriding of Zr alloys, TCM on Fundamental Aspects of Corrosion on Zr Base Alloys in Water Reactor Environments, Portland, OR, USA, IWGFPT-34, IAEA, Vienna, 1990, pp. 107–119.

[33] C. Lemaignan, J. Nucl. Mater. 187 (1992) 122.

[34] R. Salot, thesis, INP Grenoble (1996).

[35] R. Salot, F. Lefebvre, B. Barroux, C. Lemaignan, Influence of radiolysis on the oxidation kinetics of Zircaloy claddings under irradiation, 18th. Int. Symp. on Effects of Irradiation on Materials, Hyannis, MA, USA, 1997, ASTM-STP in press.

[36] H. Hayashi, K. Tsuji, T. Kogai et al., Evaluation of fuel cladding corrosion characteristics by BWR simulated corrosion loop tests, Enlarged Halden programme group meeting, Halden, Norway, Halden Project, 1996.

[37] Y. Etoh, S. Shimada, M. Sasaki, T. Kogai, H. Hayashi, M. Kitamura, K. Tsuji, M. Yamawaki, these Proceedings, p. 299.